BIOCHEMISTRY
including biophysical chemistry & molecular biology

Article

pubs.acs.org/biochemistry

Transient Kinetics and Rate-Limiting Steps for the Processive Cellobiohydrolase Cel7A: Effects of Substrate Structure and Carbohydrate Binding Domain

Nicolaj Cruys-Bagger,[†] Hirosuke Tatsumi,[‡] Guilin Robin Ren,[†,¶] Kim Borch,[§] and Peter Westh*[,†,⊥]

[†]Research Unit for Functional Biomaterials, NSM, Roskilde University, Universitetsvej 1, DK-4000 Roskilde, Denmark

[‡]Department of Chemistry, Faculty of Science, Shinshu University, Matsumoto, Nagano 390-8621, Japan

[§]Novozymes A/S, Krogshøjvej 36, DK-2880 Bagsværd, Denmark

Supporting Information

ABSTRACT: Cellobiohydrolases are exoacting, processive enzymes that effectively hydrolyze crystalline cellulose. They have attracted considerable interest because of their role in both natural carbon cycling and industrial enzyme cocktails used for the deconstruction of cellulosic biomass, but many mechanistic and regulatory aspects of their heterogeneous catalysis remain poorly understood. Here, we address this by applying a deterministic model to real-time kinetic data with high temporal resolution. We used two variants of the cellobiohydrolase Cel7A from *Hypocrea jecorina*, and three types of cellulose as substrate. Analysis of the pre-steady-state regime allowed delineation rate constants for both fast and slow steps in the enzymatic cycle and assessment of how these constants influenced the rate of hydrolysis at quasi-steady state. Processive movement on the cellulose strand advanced with characteristic times of 0.15−0.7 s per step at 25 °C, and the rate was highest on amorphous substrate. The cellulose binding module was found to raise this rate on crystalline, but not on amorphous, substrate. The rapid processive movement signified high intrinsic reactivity, but this parameter had marginal influence on the steady-state rate. This was because dissociation and association were slower and, hence, rate limiting. Specifically, the dissociation from the strand was found to occur with characteristic times of 45−100 s. This meant that dissociation was the bottleneck, except at very low substrate loads (0.5−1 g/L), where association became slower.

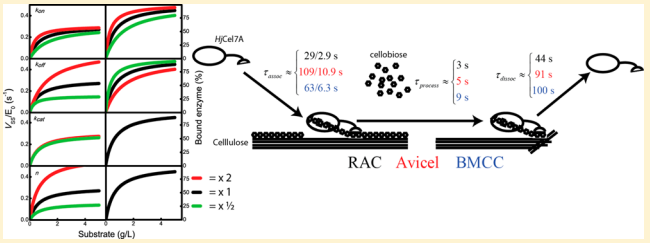

Cellulases catalyze the hydrolysis of a single type of bond (the β-1−4 glucosidic bond) in a substrate, cellulose, which is simple in the sense that it is an unbranched homopolymer and all cellulases utilize one of two catalytic mechanisms (inverting or retaining), both of which have been described in detail.[1] Nevertheless, kinetics and regulation of cellulolytic enzymes has turned out to be highly complex, and many fundamental questions remain unanswered. This scientific challenge is accompanied by a technological interest driven by the role of cellulases in emerging industries that use lignocellulosic biomass as feedstock. Thus, rational improvements of industrial enzymes and enzyme cocktails are often hampered, if not unfeasible, because of the limited fundamental understanding of the enzymatic processes. The complexity of cellulase kinetics relies at least in part on an extraordinary diversity of interactions between the enzyme and its insoluble substrate. A typical cellulase interacts strongly with the substrate both through the catalytic domain (CD) and the carbohydrate binding module (CBM).[2] In addition, recent computational studies have suggested that some glycan moieties on glycosylated cellulases also bind to the substrate interface.[3] The heterogeneous nature of the substrate adds further to the complexity because the enzymes show different affinity for different surface morphologies (e.g., different crystal allomorphs, crystal planes, or noncrystalline arrangements). The interplay between these different interactions gives rise to enzyme−substrate complexes with different structural and catalytic properties, and the conversion between such forms, which can occur on different time-scales, must be taken into account in order to describe the kinetics and identify rate limiting steps for cellulolytic enzymes.

The standard approach to elucidate separate steps in enzyme catalysis is pre-steady-state (or transient) kinetic measurements. In contrast to conventional steady-state kinetics, this can in principle quantify both rate and equilibrium constants governing individual steps in an enzyme reaction pathway.[4] To exploit this potential, however, one needs to have both an experimental technique that is fast and sensitive enough and a (realistic) model description that can be used to derive the kinetic parameters. For cellulases, these two requirements remain challenging, but the combination of real-time measurements with amperometric biosensors[5] and a simplified reaction

Received: August 31, 2013
Revised: October 12, 2013
Published: November 14, 2013

scheme for processive exocellulases (cellobiohydrolases)[6,7] has shown some promise, at least within a certain range of enzyme and substrate loads. Here, we have analyzed the rate of different steps in the catalytic cycle of the processive cellulase Cel7A from *Hypocrea jecorina* (*Hj*Cel7A). We have compared the pre-steady-state kinetics on amorphous cellulose (RAC), microcrystalline cellulose from wood (Avicel), and bacterial microcrystalline cellulose (BMCC) for both the intact *Hj*Cel7A and for a variant, *Hj*Cel7A$_{CORE}$ without the CBM and its liker. Systematic variation of both enzyme and substrate loads provided rate constants for the formation of the activated complex (k_{on}), processive catalysis (k_{cat}), and dissociation (k_{off}), respectively, as well as the processivity number, n (i.e., the average number of sequential catalytic cycles performed on one cellulose strand following each association), for these six enzyme–substrate systems. The results provide insight into the rates of each step and the effects of substrate structure and CBM on the different processes underlying the catalysis.

EXPERIMENTAL SECTION

Materials. Unless otherwise stated, all chemicals were of HPLC grade (>99% purity) and supplied by Sigma-Aldrich (St. Louis, MO). The intact retaining cellobiohydrolase, Cel7A, from *Hypocrea jecorina* (anamorph: *Trichoderma reesei*) (*Hj*Cel7A) as well as the catalytic domain alone (*Hj*Cel7A$_{CORE}$) were expressed and purified as described previously.[6,8] The purified enzymes showed a single band in SDS-PAGE, and the absence of cellobiase activity in the purified product was confirmed as the lack of detectable activity against the chromogenic substrate analogue *p*-nitrophenyl-β-D-glucopyranoside (pNPG). The protein concentration was determined from an absorbance measurement at 280 nm with the theoretical molar extinction coefficients 83 mM^{-1} cm^{-1} (*Hj*Cel7A) and 80 mM^{-1} cm^{-1} (*Hj*Cel7A$_{CORE}$) derived from the amino acid sequence. The activity at 25.0 °C of *Hj*Cel7A against 0.50 mM solutions of the soluble substrate analogue *p*-nitrophenyl β-D-lactopyranoside (pNPL) was derived from measurements at different enzyme concentrations (0–100 nM) (Cruys-Bagger et al., unpublished data). The average specific activity for the Cel7A stock used here was 3.2 ± 0.1 min^{-1}.

Cellulose Substrate Preparations. Microcrystalline cellulose (Avicel PH-101) was from Fluka. Regenerated amorphous cellulose (RAC) was prepared from Avicel by a slight modification[9] of the procedure developed by Zhang et al.[10] Bacterial microcrystalline cellulose (BMCC) from *Acetobacter xylinum* was prepared from bacterial cellulose (BC) extracted from commercially available Nata de Coco (coconut gel in syrup, Monika, Fitrite Incorporated, Novaliches Quezon City, Philippines). The method was a modification of the procedure given by Väljamäe et al.[11] The cubes were washed in deionized water at room temperature for 3 h with three water changes to remove the syrup. This was followed by alkaline treatment by three washes in 0.25 M NaOH for 3 h, followed by one wash overnight under slow continuous stirring. The cubes were then extensively washed over a period of 5 days with three water changes per day (3 days with deionized water, then 2 days with Milli-Q water) and, finally, two days' wash in the standard buffer. The suspensions were ground using a laboratory blender for 3 min until the suspension was easy to pipet. The suspension was then further homogenized using an Ultra Turrax T8 homogenizer (IKA Labortechnik, Uppsala, Sweden) for 10 min on ice. The final cellulose suspensions were stored at 4 °C after addition of 0.01% sodium azide to prevent bacterial growth. Preparations of RAC and BMCC were occasionally characterized with respect to degree of polymerization (DP) and crystallinity index I_{cr}. We used the procedure by Zhang and Lynd[12] and found DP values of 198 ± 10 and 241 ± 25 for RAC and BMCC, respectively. The crystallinity index was determined using solid-state ^{13}C cross-polarization/magic angle spinning (CP/MAS) nuclear magnetic resonance (NMR). We used previously described experimental procedures[9] and estimated the crystal content on the basis of the C-4 peak at 92–86 ppm as described by Vanderhart and Atalla.[13] We found I_{cr} of 0.87 ± 0.05 for BMCC and <0.05 for RAC.

Enzyme Assay. The concentration of cellobiose was measured in real time with cellobiose dehydrogenase-modified carbon paste electrodes as described in detail elsewhere.[5,7] The sensors offered a resolution in time and cellobiose concentration of about 1 s and 50 nM, respectively. All measurements were conducted in 50 mM sodium acetate with 2 mM $CaCl_2$ and pH 5.0 at 25 °C. We generally used substrate loads of 0–3 g/L. This was found to be several-fold more than $_pK_M$ (Table 1B) and, hence, provided essentially saturating substrate conditions.

DATA ANALYSIS

Our analysis relies on a simplified description of processive hydrolysis where the enzyme, E, attacks the end of a cellulose strand, C_m, composed of m cellobiose moieties. Each catalytic cycle then shortens the strand by one cellobiose unit (thus producing C_{m-1}, C_{m-2}, C_{m-3}, etc.) until eventually the complex dissociates after an average of n catalytic cycles. Hence, n is the processivity number. This reaction course and its rate constants for association (k_{on}), processive catalysis (k_{cat}), and dissociation (k_{off}) is illustrated in Scheme 1.

Scheme 1. Simplified Reaction Scheme for the Hydrolysis of a Cellulose Strand by a Processive Enzyme[a]

$$E + C_m \xrightarrow{k_{on}} EC_m \xrightarrow{k_{cat}} EC_{m-1} + C \xrightarrow{k_{cat}} EC_{m-2} + C\ldots \xrightarrow{k_{cat}} EC_{m-n}$$
$$\downarrow k_{off} \qquad \downarrow k_{off} \qquad \downarrow k_{off} \qquad \downarrow k_{off}$$
$$E + C_m \qquad E + C_{m-1} \qquad E + C_{m-2} \qquad E + C_{m-n}$$

[a]The enzyme, E, attacks the end of a strand, C_m, with m cellobiose units and moves processively along the strand. Cellobiose, C, is released and the strand is sequentially shortened to C_{m-1}, C_{m-2}, and so forth. The reaction is governed by four parameters: rate constants for association (i.e., formation of an activated complex), catalysis, and dissociation and a processivity number, n.

We will use two different approaches to rationalize the experimental data with respect to Scheme 1. First, we apply an expression for the temporal development of the cellobiose concentration (the so-called progress curve) to experimental data in the pre-steady-state range. Second, we use a Michaelis–Menten- (MM-) type equation that correlates the hydrolytic rate at steady state, V_{SS}, and the substrate load, S_0, in grams per liter. The latter is based on a quasi-steady-state approximation. Both of these approaches rely on the usual assumption of excess substrate (i.e., the number of attack sites on the cellulose should be much larger than the number of enzyme molecules), and both have been treated in detail elsewhere.[6,14] The mathematical expression for the progress curve, $C(t)$, is quite long and written out in the Supporting Information, eq <S2>. This expression for $C(t)$ was implemented in different nonlinear regression routines in the Mathematica 8.0 software

dx.doi.org/10.1021/bi401210n | *Biochemistry* 2013, 52, 8938–8948

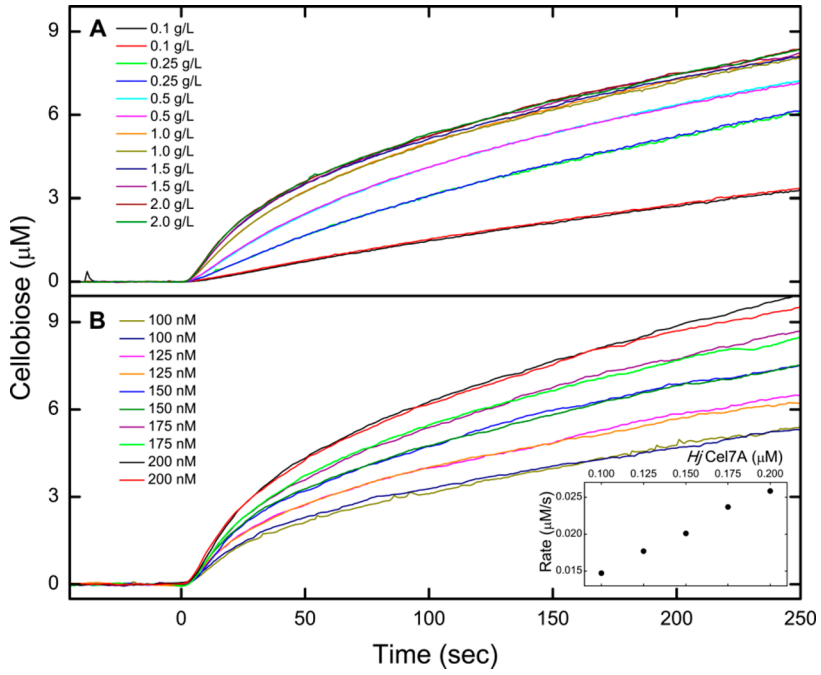

Figure 1. Representative biosensor data for the system *Hj*Cel7A-BMCC. Panel A illustrates a so-called S_0 series where the load of substrate is varied (0.1 to 2.0 g/L) and the enzyme concentration is kept constant (150 nM). Panel B shows the opposite experimental strategy (an E_0 series) where the substrate (BMCC) concentration is kept constant (3.0 g/L) and the enzyme load is varied (100 to 200 nM). Enzyme was injected at $t = 0$ as indicated by the arrow. All measurements are shown in duplicate. The insert shows the hydrolytic rate at steady state (the slope of a linear fit to the progress curve from 100 to 180 s) plotted as a function of the enzyme concentration. It appears that the rate is proportional to E_0, and this supports the assumption of excess substrate.

package (Wolfram Research, Oxfordshire, UK) and used to analyze the transient kinetic regime. At quasi-steady state (i.e., when the concentrations of the intermediates EC_m, EC_{m-1}, EC_{m-2}, etc. in Scheme 1 become almost independent of time), the rate, V_{SS}, can be written[14]

$$\frac{V_{SS}}{E_0} = \beta \frac{k_{cat} S_0}{{}_pK_M + S_0} \quad (1)$$

with

$${}_pK_M \equiv \frac{k_{off}}{k_{on}} \quad (2)$$

and

$$\beta \equiv 1 - \left(\frac{k_{cat}}{k_{cat}+k_{off}}\right)^n \quad (3)$$

Equation 1 is an analogue to the MM equation that takes processivity as defined in Scheme 1 into account. The main difference between eq 1 and the normal MM equation is the "kinetic processivity coefficient", β, which is dimensionless and always below unity. Formally, β is the probability that the activated complex will dissociate before making n-processive steps, but at saturating substrate loads, it may be interpreted as the fraction of the total enzyme population that is catalytically active.[14] In analogy to the conventional MM equation, it is useful to consider eq 1 at high and low substrate load. In the former case ($S_0 \gg {}_pK_M$), insertion into eq 1 gives an expression for the maximal specific rate at steady state, ${}^{max}V_{SS}/E_0$

$${}^{max}V_{SS}/E_0 \approx \beta k_{cat} \quad (4)$$

Conversely, consideration of $S_0 \ll {}_pK_M$ in eq 1 provides an expression for the specificity constant (or kinetic efficiency), ${}_p\eta$, for processive catalysis (i.e., the slope of eq 1 at very low S_0)

$${}_p\eta = \beta \frac{k_{cat}}{{}_pK_M} \quad (5)$$

RESULTS

Representative raw data from the electrochemical biosensor measurements are illustrated in Figure 1. In this example, we used the intact *Hj*Cel7A enzyme and BMCC. Panel A shows a series of measurements with a constant enzyme concentration (150 nM) and variable substrate loads ranging from 0.1 to 2 g/L. Henceforth, we will call this a S_0 series because the substrate load, S_0, is varied. Panel B illustrates an example of the opposite experimental strategy where the enzyme concentration was varied from 100 to 200 nM in steps of 25 nM, while the substrate (BMCC) was kept constant at 3.0 g/L (a so-called E_0 series). Two separate runs are shown for each enzyme and substrate load to illustrate the experimental reproducibility. The slope of these traces, that is, the rate of hydrolysis, reached a maximum soon after the injection of enzyme (at $t = 0$ s). The location of this inflection point on the progress curve depended on the substrate loads (it occurred earlier the higher the loads) and fell in the range 4−7 s for RAC and 5−12 s for Avicel and BMCC. Subsequently, the slopes leveled off quickly and reached a near-linear course after about 60 s for RAC and 100 s for the more crystalline substrates Avicel and BMCC. This near-linear course was interpreted as a pseudo-steady-state condition. A distinctive initial burst as described above was observed for all enzyme concentrations in the E_0 series with high substrate load (Figure 1B). Conversely, in the S_0 series, the

dx.doi.org/10.1021/bi401210n | *Biochemistry* 2013, 52, 8938−8948

burst gradually tapered off with decreasing loads, and almost linear progress curves were observed for the lowest S_0 (Figure 1A). These general traits, illustrated for *Hj*Cel7A-BMCC in Figure 1, were also found for the *Hj*Ce7A$_{CORE}$ variant and for the other types of substrate studied here (see examples in the Supporting Information). The slope of the progress curves in Figure 1B in the near-linear range (100 s < t < 180 s) is plotted as a function of the enzyme concentration, E_0, in the insert of this figure. This shows that the hydrolytic rate scaled proportionally with E_0 and this supports the assumption that the substrate is in excess. Similar behavior was observed for the other enzyme−substrate systems. Figures 1−3 show that the highest cellobiose concentrations were ∼10 μM, and this is about 2 orders of magnitude lower than published cellobiose inhibition constants (or IC$_{50}$ values) for Cel7A hydrolyzing insoluble cellulose.[15−17] Hence, we will neglect product inhibition in the subsequent analysis.

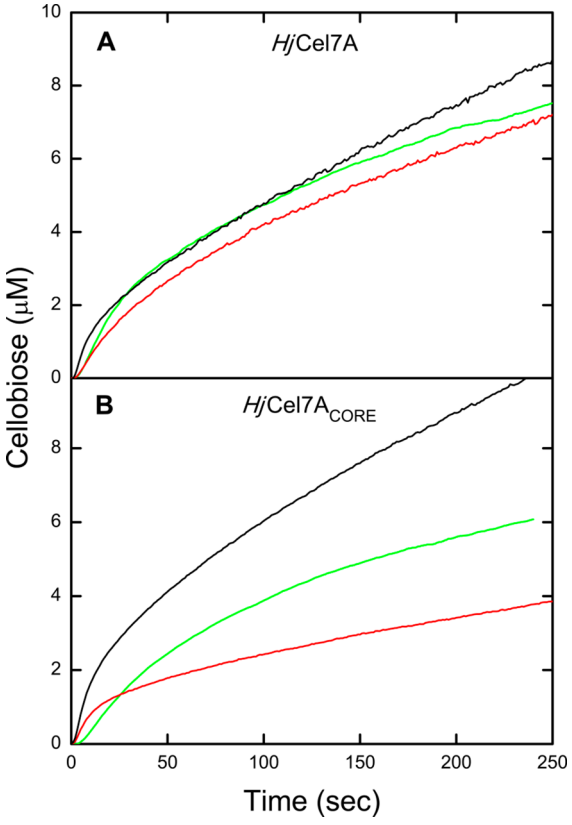

Figure 2. Illustration of differences in progress curves for different combinations of enzyme and substrate. All measurements were conducted with 150 nM enzyme and 3.0 g/L substrate using either the intact *Hj*Cel7A (Panel A) or the truncated *Hj*Cel7A$_{CORE}$ variant (Panel B). Black, red, and green traces are for RAC, Avicel, and BMCC, respectively.

Comparisons of the continuous experiential data provide a way to assess the rate of different steps in the enzymatic reaction. Before turning to explicit modeling, this was empirically illustrated in Figure 2, which shows progress curves for the three substrates and two enzyme variants at fixed loads of 150 nM enzyme and 3.0 g/L substrate. It appears that quite different progress curves were observed and that crossovers were not uncommon. The *Hj*Cel7A$_{CORE}$ variant, for example, showed a high initial activity on Avicel (red trace in Figure 2B), and at t = 10 s the amount of released cellobiose is over twice

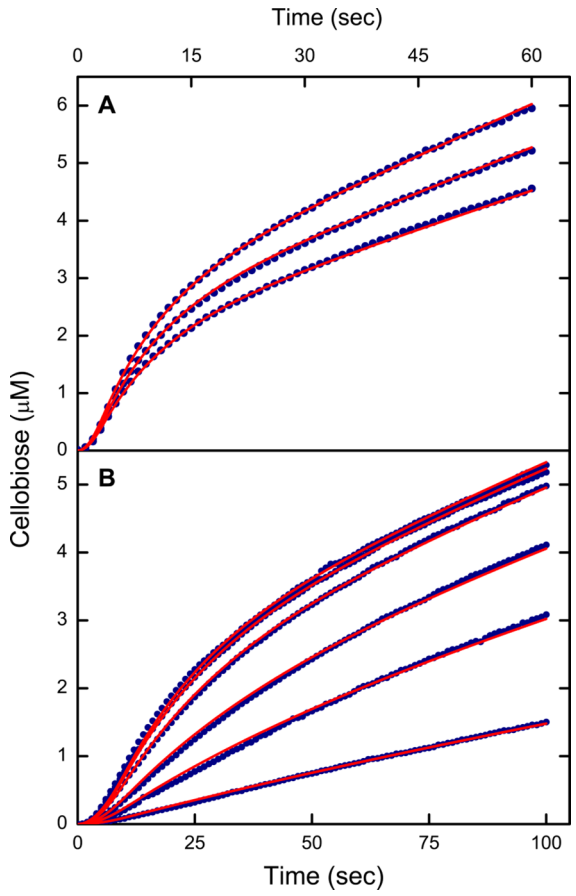

Figure 3. (A) Global nonlinear regression of data for the *Hj*Cel7A$_{CORE}$−RAC system. In this E_0 series we used 150, 175, and 200 nM enzyme and 3.0 g/L substrate. (B) Global nonlinear regression with local on-rate constant (k_{on}) for a S_0 series using BMCC (0.10. 0.25, 0.50, 1.0, 1.5, and 2 g/L) and a constant *Hj*Cel7A concentration of 150 nM. Circles represent experimental data points and lines are the best global nonlinear regression fit.

the value for BMCC (green). However, at pseudo-steady state, BMCC hydrolysis is faster, and after 3 min, the release from BMCC is 65% higher compared to Avicel. A qualitatively similar behavior was seen for the intact enzyme (Figure 2A), but in this case, the differences between the three substrates were much smaller.

Figure 2 provides a qualitative illustration of differences between progress curves, and to study this systematically, we analyzed all data with respect to Scheme 1. First, we used nonlinear regression of eq <S2> from the Supporting Information to analyze the progress curves in the pre-steady-state regime. As in any pre-steady-state study, care must be taken when selecting the time range for the regression analysis. For cellulases, this is relevant because a loss of activity (unrelated to the processes in Scheme 1) has been shown to develop on slower time scales.[18] To minimize the influence of this, we only used data up to the point where quasi-steady-state is established[6,7] (i.e., the intervals 0−60 s for RAC and 0−100 s for Avicel and BMCC) in the regressions. It was found that eq <S2> accounted very well for experimental data when single runs were analyzed. To further test the applicability, we also implemented different types of global analyses that simultaneously fitted a collection of runs in either E_0 or S_0 series. This is a more discriminatory approach because it requires that a

dx.doi.org/10.1021/bi401210n | *Biochemistry* 2013, 52, 8938−8948

Table 1. Maximum Likelihood Parameters and Derived Parameters, Including Steady-State Kinetics Constants[a]

	RAC		Avicel		BMCC	
	*Hj*Cel7A	*Hj*Cel7A$_{Core}$	*Hj*Cel7A	*Hj*Cel7A$_{Core}$	*Hj*Cel7A	*Hj*Cel7A$_{Core}$
Panel A						
k_{on} ((g/L)$^{-1}$ s^{-1})[b]	0.035	0.034	0.0092	0.031	0.016	0.012
k_{cat} (s^{-1})	5.1	6.5	4.75	3.9	2.4	1.4
k_{off} (s^{-1})	0.023	0.020	0.011	0.011	0.010	0.012
n	13.7	18.6	22.7	9.4	22.6	20.5
Panel B						
n_{theo}[c]	222	325	432	355	240	115
β[d]	0.060	0.056	0.051	0.026	0.090	0.16
$^{max}V_{SS}/E_0$ (s^{-1})[e]	0.30	0.36	0.24	0.10	0.22	0.23
$_pK_M$ (g/L)	0.66	0.59	1.20	0.35	0.63	1.01
$_p\eta$ ((g/L)$^{-1}$ s^{-1})[f]	0.46	0.61	0.20	0.29	0.34	0.22

[a]Panel A shows kinetic parameters derived from nonlinear regression. We used eq <S.2> (Supporting Information) and the pre-steady-state progress curves as exemplified in Figure 3. The parameters are for the intact enzyme (*Hj*Cel7A) or its catalytic domain (*Hj*Cel7A$_{CORE}$) and for three different substrates: RAC, Avicel, and BMCC. All data are for T = 25 °C and pH = 5.0. Panel B shows the theoretical processivity (n_{theo}) and a number of steady-state kinetic parameters calculated from the rate constants and processivity in panel A. These derived parameters are calculated according to eqs 1−6, and some supporting comments are given in the footnotes *b*−*f*. [b]For S_0 = 3.0 g/L [c]The theoretical processivity, n_{theo}, is the number of sequential steps the enzyme would statistically make on a long, perfectly regular substrate strand (see eq 6). [d]β is the kinetic processivity coefficient (see eq 1) and equals the fraction of active enzyme at saturated substrate load. [e]The maximal specific activity (i.e., V_{SS}/E_0 at saturating substrate loads) was calculated from eq 4. [f]$_p\eta = \beta k_{cat}/_pK_M$ is the substrate specificity for a processive reaction (i.e., the slope of eq 1 at very low S_0). It was calculated from eq 5.

single set of parameters accounts for a larger data set (it is a three-dimensional analysis). Results of this consistently showed that E_0 series could be globally reproduced by eq <S2>, and an example is shown in Figure 3A. Conversely, global analysis of S_0 series (constant enzyme concentration and different substrate loads) did not show good fits. However, if a S_0 series was analyzed with k_{on} as a local parameter (i.e., allowing a separate k_{on} value for each experiment in the regression) and k_{cat}, k_{off}, and n as global parameters for the whole S_0 series, we obtained both good fits (Figure 3B) and the same values of k_{cat}, k_{off}, and n as in the E_0 series.

We conclude that for each enzyme−substrate system, global values of the parameters k_{cat}, k_{off}, and n can be retrieved from a broad set of data with variable enzyme and substrate loads. The on-rate constant, which is a composite constant that lumps together the steps leading from enzyme in aqueous solution to the formation of an activated complex, varies with the substrate (but not the enzyme) load. We will return to this and its possible underpinnings below. The maximum likelihood parameters from the regression analysis are listed in Table 1A. For k_{on}, the value in Table 1A is for a substrate load of 3 g/L. All parameters in Table 1A are to be considered ensemble averages because rate constants and processivities will vary with the local environment of specific cellulose chains. Some derived parameters, which can be calculated from the values in Table 1A, are useful in discussions of different aspects of the enzymatic process. These derived parameters, which include the steady-state kinetics constants defined in eq 1−5, are listed in Table 1B.

Some of the parameters in Table 1A can be compared to literature data on *Hj*Cel7A kinetics, and in general, the accordance with previous work is good. For example, the rate of *Hj*Cel7A's movement on crystalline cellulose (3.5−7.1 nm/s) measured by high speed AFM[19,20] corresponds to the processive rate stipulated by the current k_{cat} values (as one cellobiose moiety is about 1.0 nm long). Also, biochemical measurement of the enzyme's maximal specific rate (~1.8 s^{-1} and 2.2−2.8 s^{-1} for amorphous cellulose and bacterial cellulose, respectively)[21,22] fell in the same range as the k_{cat} values in Table 1A. Different measurements of the processivity for this enzyme on labeled amorphous cellulose (20.8)[21] and bacterial cellulose (42)[23] are in reasonable accord with the n values found here, and the processivities on amorphous cellulose derived from product profiles (n values of 14 to 23) also match the values in Table 1A very well.[24] Processivities from the literature generally show the same tendency toward higher values for more crystalline substrates, as seen here. The off-rate has been measured on labeled amorphous cellulose to 0.0032 s^{-1}.[21] This is almost an order of magnitude lower than the value in Table 1A for RAC. We cannot explain this difference, but it could rely on different types of materials used for the preparation of amorphous cellulose.

DISCUSSION

Identification of the rate-limiting step in the complex catalytic cycle of processive cellulases is of direct interest in different areas, both scientific and technological. For example, it could potentially pave the way for rational modification of catalytic properties of enzymes used in biomass treatment. However, it has proven difficult to designate the molecular underpinnings of the rate determination, and recent works have been divisive and emphasized association,[25−28] dissociation,[7,21,29] or substrate decrystallization[30−32] as major bottlenecks. Here, we address this in a quantitative way by breaking the cellulolytic cycle into steps that can be kinetically distinguished in the pre-steady-state regime. The analysis is simplified in the sense that the reactions in Scheme 1 do not provide a detailed account of the process but assemble different potential steps into one reaction. For example, the association step in Scheme 1 takes the enzyme directly from the aqueous bulk to the state of an activated complex, although this process might arguably be split into smaller steps such as adsorption, surface diffusion, and chain acquisition.[22,33,34] As a result, the rate constants obtained here are composite constants that describe the aggregate kinetics of going through these steps without any ability to resolve finer levels of transformation. We tested some more detailed reaction

schemes but consistently found that they suffered from overparameterization when experimental data was analyzed, and we decided to stay with the simpler description of Scheme 1. Some of the limitations of a simplified reaction scheme were outweighed by studying six different enzyme−substrate systems, thus bringing comparative arguments into the discussion of rate limitation. In the following, we discuss each parameter from Table 1 separately.

Catalytic Rate Constant. The first order rate constant, k_{cat}, specifies the (mean) rate of processive movement after the activated complex has been formed. Hence, it provides a measure of the "intrinsic reactivity"[35] by taking nonreacting (free or stalled) enzyme populations into account. Table 1A shows that the highest values of k_{cat} (5−7 s^{-1}) were observed on the amorphous substrate, RAC, and that the CBM had a slight negative effect on k_{cat} for this substrate. It is interesting to compare k_{cat} and ${}^{max}V_{SS}/E_0$ (see eq 4). For simple MM−enzyme kinetics, these two parameters are equal, but for the current systems, the maximal specific rate is consistently much lower than k_{cat}. If we again use RAC−*Hj*Cel7A as an example, ${}^{max}V_{SS}/E_0$ was 0.30 s^{-1} and, hence, 15−20 times less than k_{cat}. Even in the burst phase, when the hydrolysis is faster than at steady state the specific rate on RAC did not exceeded 1 s^{-1}. The immediate implication of this is that the catalytic cycle is not rate limiting. For Avicel, k_{cat} showed intermediate values and for the most crystalline substrate investigated here, BMCC, k_{cat} (1.4−2.4 s^{-1}) was less than half the value for RAC. This implies that processive movement is faster on a more disordered substrate, possibly because less work is required to release a strand from the cellulose particle. In spite of the clear differences in k_{cat}, the observation that ${}^{max}V_{SS}/E_0 \ll k_{cat}$ suggested that variations as in Table 1A are unimportant for the rate of cellobiose production at quasi-steady state, V_{SS}. This again reflects that the catalytic cycle is fast compared to other steps in the reaction and, hence, is not critical with respect to rate limitation at steady state. This is further illustrated in Figures 5 and 6, which show examples of parameter dependence for the *Hj*Cel7A/RAC system. It appears from Figure 6 that V_{SS}/E_0 is essentially unchanged when k_{cat} is increased or diminished by a factor of 2. A similar low sensitivity of V_{SS} to k_{cat} was found for the other enzyme−substrate systems, and we conclude that although the enzyme moved faster on the more disordered substrate, this had almost no effect on the activity at steady state. This clearly suggests that the activation energy associated with decrystallization of cellulose was not rate limiting at steady state under the conditions studied here. Turning to the effect of the CBM, we compared k_{cat} values for the intact enzyme (*Hj*Cel7A) and the *Hj*Cel7A$_{CORE}$ variant. This comparison showed that the CBM increased the rate of processive movement on crystalline substrates (BMCC and Avicel) but not on amorphous RAC. The molecular mechanism underlying this cannot be unequivocally established, but we note that the CBM has previously been suggested to facilitate hydrolysis through a disruptive effect on cellulose crystal structure.[36,37] This would be in line with the observation that the CBM only promotes k_{cat}, and hence the rate of processive movement, on substrates with an appreciable crystalline content (BMCC and Avicel). The lack of a positive effect on the hydrolysis of RAC may also simply reflect that the CBM of Cel7A has a very low affinity for amorphous cellulose.[38] Earlier studies have shown that the CBM strongly promotes the overall activity on Avicel, though its effect on the hydrolysis of amorphous cellulose is marginal.[39] This mirrors the effects of the CBM on k_{cat} reported here, and it is tempting to suggest that the inefficient hydrolysis of crystalline substrates by *Hj*Cel7A$_{CORE}$ is caused by its lower k_{cat}. However, the results do not support this interpretation because the catalytic step is not rate limiting. We conclude that the CBM indeed brings about faster processive movement on crystalline substrates, but in analogy to the case of different substrate types (discussed above), these moderate changes in k_{cat} have essentially no effect on V_{SS}. We will return to the role of the CBM below when the other parameters are discussed. To summarize, we found that processive catalysis was much faster (1−7 s^{-1}) than the maximal specific activity at steady state (0.1−0.4 s^{-1}), and this illustrates the potential of the current approach. Thus, modeling of transient kinetics allows delineation of steps that are considerably faster that the observed rate of reaction, as well as information on how this fast step is affected by substrate type and the CBM. Specifically, k_{cat} values in Table 1A suggest the following: (i) The processive movement is faster on a disordered substrate, possibly due to less work of chain ablation. (ii) The CBM increases the rate of processive movement on crystalline, but not on amorphous, substrate. This, again, could rely on the activation energy associated with decrystallization, which may be lowered through CBM binding. (iii) Both effects described in (i) and (ii) have marginal impact on the rate of hydrolysis at steady state because k_{cat} is not rate limiting under the investigated conditions.

Off Rate Constant and Processivity. The other first order rate constant in Table 1A, k_{off}, governs the dissociation of the enzyme−substrate complexes in Scheme 1. This parameter is more than hundred-fold smaller than k_{cat}, and if we express this in terms of half-lives (ln 2/k) of the two processes, the values range from 30−70 s for dissociation and 0.1−0.5 s for catalysis. This marked difference is a hallmark of the enzyme's processivity because it implies that, statistically, *Hj*Cel7A will make many catalytic steps before it dissociates. One convenient way to quantify this is through the so-called theoretical (or intrinsic) processivity, n_{theo}, which can be expressed by the on and off rate constants.[40] Provided that $k_{cat} \gg k_{off}$ (as is indeed the case here), we may write

$$n_{theo} \approx \frac{k_{cat}}{k_{off}} \tag{6}$$

This statistical parameter specifies the average expected number of consecutive catalytic steps if the process was solely governed by the probabilities of respectively catalysis and dissociation (c.f. Scheme 1). This number was 100−400 (Table 1B) for the investigated systems and, hence, much higher than the experimental processivities (n = 14−23, Table 1A). This discrepancy has been reported before and interpreted as the result of irregularities or "obstacles" on the cellulose surface, which hampers processive movement.[21] In other words, the processive sweep is (on average) stopped long before the enzyme would randomly dissociate from the strand. As a result, slow dissociation (dictated by the low k_{off}) of enzyme stalled in front of such obstacles becomes limiting for the rate at steady state. This can be quantified at saturating substrate loads. Thus, under the premises that $k_{cat} \gg k_{off}$ and $S_0 \gg {}_pK_M$, eq 1 reduces to the approximate relation $V_{SS}/E_0 \approx k_{off}n$.[14] The strong dependence (near-proportionality) of the specific rate on both k_{off} and n predicted by this equation is also illustrated in Figure 6, where manipulation of these two parameters are shown to

dx.doi.org/10.1021/bi401210n | *Biochemistry* 2013, 52, 8938−8948

strongly modify the steady-state hydrolysis rate, and we conclude that the (low) k_{off} value is a major determinant of the overall activity. Low processivity, which is interpreted as a limited obstacle-free path length on the substrate, is equally important. It is interesting to note that k_{off} is essentially unaffected by the CBM for all three substrates (*Hj*Cel7A and *Hj*Cel7A$_{CORE}$ have similar values for each substrate in Table 1A). This suggests that the main energy barrier for dissociation is the release of the cellulose strand from the catalytic domain. This interpretation is in line with a recent single-molecule fluorescence imaging study,[41] which proposed that a biphasic decay pattern for *Hj*Cel7A binding times reflected slow release of the catalytic domain and faster release of the population with only the CBM attached. The release dynamics found here were faster for an amorphous substrate (RAC, k_{off} = 0.02 s^{-1}) than for Avicel and BMCC (k_{off} = 0.01 s^{-1}), and this difference (rather than the difference in k_{cat} discussed above) is a main reason for the lower steady-state activity on the two more crystalline substrates. Mechanistic discussions of the faster dissociation from amorphous substrate awaits further investigations, but effects from remaining phosphate substituents added during the preparation of RAC cannot be ruled out, although such substituents have been reported to be rare.[10]

Association Rate Constant. The last parameter in Table 1A, k_{on}, governs the rate of forming the activated complex EC_m in Scheme 1. This second order constant was defined[6] in the expression for the rate of association $d[EC_m]/dt = k_{on}[E]S_0$. This is a conventional definition (based on mass action kinetics) that implies that the association shows first-order kinetics with respect to both the concentration of enzyme and substrate. However, as pointed out in the Results section, it was found that one on rate constant defined in this way could not fit all data in an S_0 series (constant enzyme–variable substrate). Conversely, good fits could be obtained with a global k_{on} value in E_0 series. For the S_0 series, we consistently found decreasing k_{on} values as the substrate load rose. Figure 4 shows some

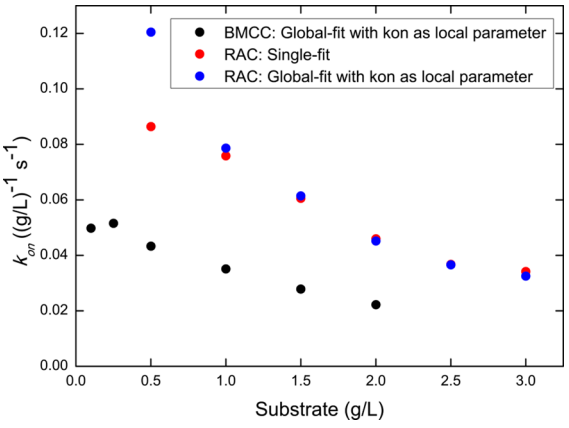

Figure 4. Maximum likelihood values for k_{on} derived either from fits to single experiments or global analysis of S_0 series with k_{on} as a local parameter (c.f. Figure 3B). The tendency for k_{on} to decrease with S_0 was found throughout this work.

examples of this, and we conclude that the simple mass action approach does not capture the association kinetics when S_0 is varied. In other words, the association process appears to exhibit first order kinetics with respect to the enzyme, but not the substrate, load. This may rely on the insoluble (and, hence, nondiffusive) nature of the substrate, and it has been suggested that because of this, the problem may be better rationalized by the theory of fractal kinetics.[42−44] Although an examination of fractal kinetics is beyond the current scope, we note that all experimental data here is obtained at negligible degrees of substrate conversion. This means that the number of attack sites for the cellulase will be proportional to the load of substrate. The constant of proportionality that defines the number of attack sites per mass unit of substrate is unknown (and different for each type of substrate), but this constant will be built into the rate constant k_{on} when the latter is given in mass-based units as in Table 1A. Therefore, it appears reasonable to expect first-order behavior with respect to the substrate load at very low degrees of conversion. Indeed, this simple mass-action approach for the on rate has been widely and successfully used for the kinetic description of Langmuir-type adsorption to (nonreacting) solid surfaces.[45] In light of this, we speculate that the decreasing values of k_{on} in Figure 5 could rely on factors other than the nondiffusivity of the substrate. One possibility could be attractive forces between cellulose particles,[46] which would gradually promote interactions and, hence, reduce the effective surface area per gram substrate as S_0 increased. This interpretation is also in line with adsorption data obtained for variable S_0. Hence, Wang et al.[47] found that both the apparent affinity constant and the saturation coverage (in milligrams of cellulase per gram of cellulose) for the adsorption of mixed cellulases to Avicel decreased with increasing cellulose load. This is in contrast to simple Langmuir theory and could be explained by a nonadditivity arising from mutual attraction between the particles.

As discussed above, k_{on} values incorporate an unknown factor that specifies the number of enzyme attack points per mass unit of substrate. This factor will vary with the substrate type, and it follows that k_{on} values for different substrates cannot be readily compared. Comparisons of different enzyme variants on the same substrate, however, might be relevant. Applying this perspective to Table 1A shows that k_{on} is almost unaffected by the CBM for both RAC and BMCC. For Avicel, on the other hand, k_{on} is much higher for *Hj*Cel7A$_{CORE}$ than for the intact enzyme. This implies that formation of activated enzyme–Avicel complex occurs faster without the CBM, and this behavior is directly illustrated in Figure S4 (Supporting Information). Thus, although the intact enzyme hydrolyses Avicel almost twice as fast as *Hj*Cel7A$_{CORE}$ at steady state, the CORE variant is much faster over the first few seconds. This rapid start is a hallmark of high k_{on}, but the molecular origin of this behavior remains obscure.

Parameter Variation. It appears from Table 1A that the parameters typically vary by a factor of 2–3 between the different substrates types and enzyme variants studied here. To illustrate how variations of this magnitude modify the enzymatic process, we have estimated activity and adsorption in a number of hypothetical cases. The mathematical underpinnings are given in the Supporting Information. We chose the parameters for *Hj*Cel7A–RAC in Table 1A as the starting point and first calculated the cellobiose progress curve and the time course of enzyme adsorption. These two functions are plotted in black in respectively the left- and right-hand columns of Figure 5 (the black curves within each column are identical). Next, we artificially changed one parameter by a factor of 2 (red curves) or a factor of 1/2 (green curves) and left the other three unchanged. The results in the four rows of Figure 5 illustrate how the temporal development of the

dx.doi.org/10.1021/bi401210n | *Biochemistry* 2013, 52, 8938−8948

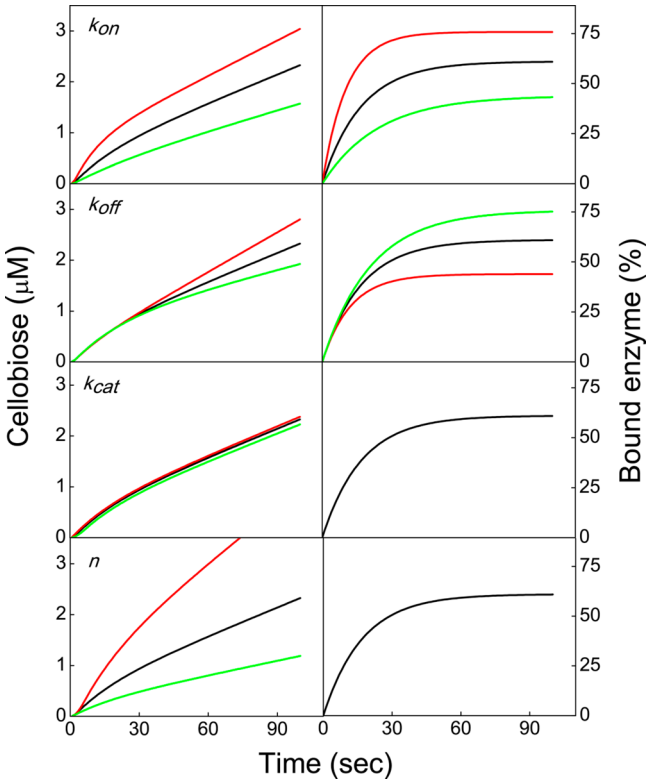

Figure 5. Effects of parameter manipulation on progress curves (left column) and adsorption kinetics (right column). Curves in black are calculated on the basis of the parameters for the *Hj*Cel7A-RAC system (Table 1A). Red and green curves show the results of doubling and halving, respectively, the indicated parameter while keeping the other three parameters constant. For the lower two plots in the right-hand column, the three curves are superimposed (signifying independence of the parameter).

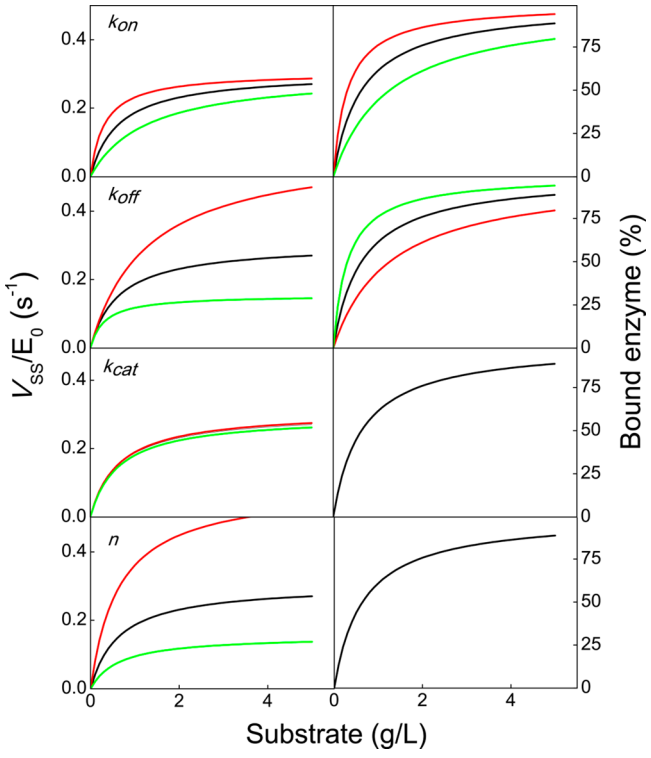

Figure 6. Effects of parameter manipulation on the steady-state levels of the specific activity (left column) and enzyme adsorption (right column). The color coding is the same as in Figure 5

cellobiose concentration (left) and enzyme adsorption (right) is predicted to vary with each of the parameters. The same type of analysis was also conducted for the apparent specific rate (V_{SS}/E_0) and adsorption at steady state and plotted as a function of the substrate load in Figure 6. Several insights of the kinetics can be derived from these plots. We have already discussed the observation that changes in k_{cat} exert almost no effect on the hydrolytic rate. Regarding this parameter, we also found that it had no effect on the adsorption, which was entirely governed by k_{on} and k_{off} (all three curves in the two lower panels to the right in Figures 5 and 6 are superimposed). Doubling k_{on} generated a much faster association and more pronounced initial burst (Figure 5) but had little effect on the hydrolytic rate at longer times or higher substrate loads (Figures 5 and 6). Increment of k_{off} essentially showed the opposite effect. Thus, calculated curves with $2 \times k_{off}$ showed a less conspicuous burst phase but a higher hydrolytic rate at steady state (except at very low substrate loads). It is interesting to compare adsorption and activity data in this case. Thus, at steady state (Figure 6), we found that although a doubling of k_{off} markedly reduced the fraction of associated enzyme, it increased the catalytic rate. This may appear paradoxical, but it simply reflected that dissociation was rate determining. Therefore, the dominant consequence of increasing k_{off} is a shorter delay for the release of stalled enzyme, which has completed a processive run. The absolute population of adsorbed enzyme is less important. To elucidate this, it is useful to note that "adsorbed" in the sense of Scheme 1 means that the enzyme is in one of the intermediates EC_m, EC_{m-1}, EC_{m-2}, ..., EC_{m-n}. All except the last of these intermediates are catalytically active (i.e., the population $\sum_{i=0}^{i=n-1}[EC_{m-i}]$), while the last (dissociating) EC_{m-n} intermediate is not. As illustrated in the Supporting Information, an increase of k_{off} primarily brings about a lower population of this inactive intermediate, and this, in turn, causes higher activity although the total adsorbed population declines. The observation that adsorption and activity of cellulolytic enzymes may be decoupled has also been repeatedly suggested on the basis of activity measurements.[30,48] The data in Figures 5–6 and the Supporting Information provide some new insight into the molecular mechanistic of this decoupling on short time-scales, but we emphasize that other effects including enzyme stability issues may become increasingly important as the hydrolysis progresses.

Summary. We have made continuous measurements of the activity of *Hj*Cel7A and the variant *Hj*Cel7A$_{CORE}$ at 25 °C on three substrates with a time resolution of about 1 s.[5] The results were analyzed against a deterministic kinetic model for processive hydrolysis, which had previously been solved with respect to both transient and quasi-steady-state kinetics. This analysis allowed us to delineate the time scale for different steps of the enzymatic process and to assess how changes in the rate of these steps would affect the hydrolysis rate at steady state. Figure 7 provides a graphical overview of some of the results. The three columns of numbers in both panels A and B give characteristic times, τ, for the formation of an activated complex, $\tau_{assoc} = 1/k_{on}S_0$, the completion of one (average) processive sweep with n steps, $\tau_{process} = n/k_{cat}$, and for dissociation, $\tau_{dissoc} = 1/k_{off}$. The values are for the substrates RAC (black), Avicel (red), and BMCC (blue), and panels A

dx.doi.org/10.1021/bi401210n | *Biochemistry* 2013, 52, 8938–8948

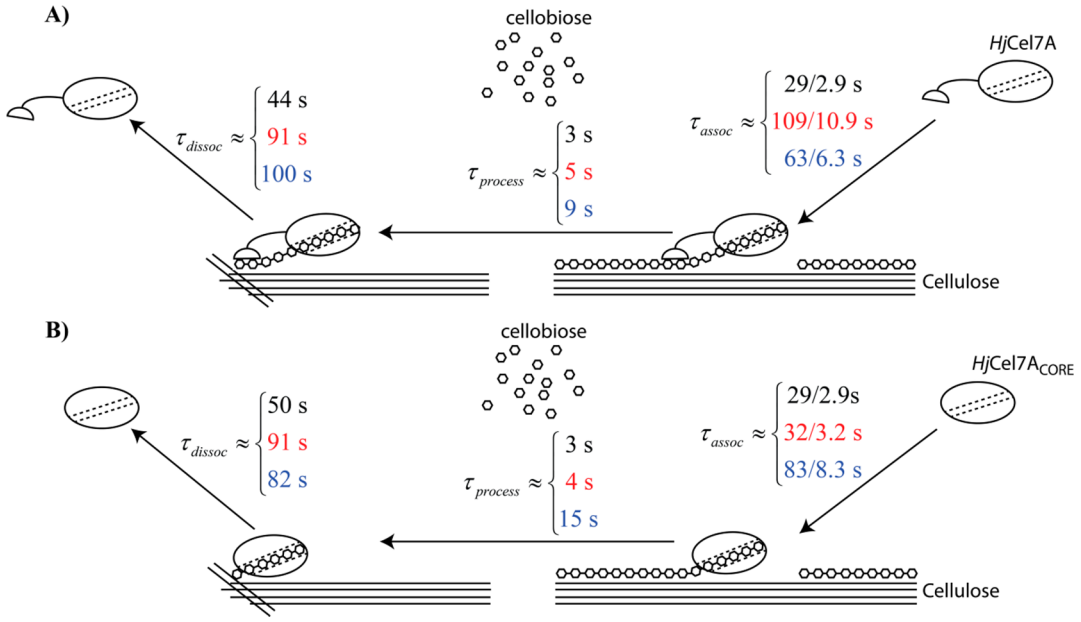

Figure 7. Illustration of characteristic times for (i) formation of an activated complex (τ_{assoc}), (ii) a processive run of n steps ($\tau_{process}$), and (iii) dissociation (τ_{dissoc}). The first step (association) depends on the substrate load and τ_{assoc} is given for 1 and 10 g/L. Black, red, and blue numbers are for RAC, Avicel, and BMCC, respectively.

and B illustrate *Hj*Cel7A and *Hj*Cel7A$_{CORE}$, respectively. The first step depends strongly on the concentration of substrate and values are given for 1 and 10 g/L, respectively. We found that a processive sweep (9−23 hydrolytic steps) was completed within 3−15 s and that this was in general as fast or faster than the two other processes. At high substrate load, the dissociation is clearly the slowest step, but if the substrate is reduced to a load around the $_pK_M$ value (c.f. eq 2 and Table 1B), τ_{assoc} approaches τ_{dissoc} and, hence, both formation of the activated complex and dissociation will become relevant to rate determination. At still lower substrate loads, formation of the activated complex will be rate limiting.

■ ASSOCIATED CONTENT

Supporting Information

Additional experimental data from the enzyme biosensor measurements, analytical solutions for the time-dependent rate and concentration of cellobiose to Scheme 1, and analytical solutions for the time-dependent and steady-state enzyme distributions together with parameter variation simulation of the enzyme population. This material is available free of charge via the Internet at http://pubs.acs.org.

■ AUTHOR INFORMATION

Corresponding Author

*P. Westh. E-mail: pwesth@ruc.dk.

Present Addresses

[¶]Department of Biology, Cell Biology and Neurobiology, Copenhagen University, Universitetsparken 15, DK-2100, Denmark.

[⊥]Research Unit for Functional Biomaterials, NSM, Roskilde University, Universitetsvej 1, 4000 Roskilde, Denmark. Telephone: (+45) 4674-2879. Fax: (+45) 4674-3011.

Funding

This work was supported by the Danish Agency for Science, Technology and Innovation, Programme Commission on Sustainable Energy and Environment (grant # 2104-07-0028 to P.W.) and the Ministry of Education, Culture, Sports, Science and Technology in Japan (grant-in-aid for young scientists # 23760746 and special coordination funds for promoting science and technology to H.T.).

Notes

The authors declare the following competing financial interest(s): Novozymes is a major enzyme-producing company.

■ REFERENCES

(1) Withers, S. G. (2001) Mechanisms of glycosyl transferases and hydrolases. *Carbohydr. Polym. 44*, 325−337.

(2) Teeri, T. T. (1997) Crystalline cellulose degradation: New insight into the function of cellobiohydrolases. *Trends Biotechnol. 15*, 160−167.

(3) Taylor, C. B., Talib, M. F., McCabe, C., Bu, L. T., Adney, W. S., Himmel, M. E., Crowley, M. F., and Beckham, G. T. (2012) Computational Investigation of Glycosylation Effects on a Family 1 Carbohydrate-binding Module. *J. Biol. Chem. 287*, 3147−3155.

(4) Johnson, K. A. (1992) Transient-state kinetic analysis of enzymes reaction pathways in *The Enzymes: Mechanisms of Catalysis* (Sigman, D. S., Ed.) 3rd ed., Academic Press Inc.: Salt Lake City, UT

(5) Cruys-Bagger, N., Ren, G., Tatsumi, H., Baumann, M. J., Spodsberg, N., Andersen, H. D., Gorton, L., Borch, K., and Westh, P. (2012) An amperometric enzyme biosensor for real-time measurements of cellobiohydrolase activity on insoluble cellulose. *Biotechnol. Bioeng. 109*, 3199−3204.

(6) Praestgaard, E., Elmerdahl, J., Murphy, L., Nymand, S., McFarland, K. C., Borch, K., and Westh, P. (2011) A kinetic model for the burst phase of processive cellulases. *FEBS J. 278*, 1547−1560.

(7) Cruys-Bagger, N., Elmerdahl, J., Praestgaard, E., Tatsumi, H., Spodsberg, N., Borch, K., and Westh, P. (2012) Pre-steady-state Kinetics for Hydrolysis of Insoluble Cellulose by Cellobiohydrolase Cel7A. *J. Biol. Chem. 287*, 18451−18458.

(8) Baumann, M. J., Borch, K., and Westh, P. (2011) Xylan oligosaccharides and cellobiohydrolase I (TrCeI7A) interaction and effect on activity. *Biotechnol. Biofuels 4*, No. 10.1186/1754-6834-4-45.

(9) Murphy, L., Baumann, M. J., Borch, K., Sweeney, M., and Westh, P. (2010) An enzymatic signal amplification system for calorimetric studies of cellobiohydrolases. *Anal. Biochem. 404*, 140−148.

(10) Zhang, Y. H. P., Cui, J. B., Lynd, L. R., and Kuang, L. R. (2006) A transition from cellulose swelling to cellulose dissolution by o-phosphoric acid: Evidence from enzymatic hydrolysis and supramolecular structure. *Biomacromolecules 7*, 644−648.
(11) Väljamäe, P., Sild, V., Nutt, A., Pettersson, G., and Johansson, G. (1999) Acid hydrolosis of bacterial cellulose reveals different modes of synergistic action between cellobiohydrolase I and endoglucanase I. *Eur. J. Biochem. 266*, 327−334.
(12) Zhang, Y. H. P., and Lynd, L. R. (2005) Determination of the number-average degree of polymerization of cellodextrins and cellulose with application to enzymatic hydrolysis. *Biomacromolecules 6*, 1510−1515.
(13) Vanderhart, D. L., and Atalla, R. H. (1984) Studies of microstructure in native celluloses using solid-state C-13 NMR. *Macromolecules 17*, 1465−1472.
(14) Cruys-Bagger, N., Elmerdahl, J., Praestgaard, E., Borch, K., and Westh, P. (2013) A steady state theory for processive cellulases. *FEBS J. 280*, 3952−3961.
(15) Murphy, L., Bohlin, C., Baumann, M. J., Olsen, S. N., Sorensen, T. H., Anderson, L., Borch, K., and Westh, P. (2013) Product inhibition of five Hypocrea jecorina cellulases. *Enzyme Microb. Technol. 52*, 163−169.
(16) Gruno, M., Väljamäe, P., Pettersson, G., and Johansson, G. (2004) Inhibition of the Trichoderma reesei cellulases by cellobiose is strongly dependent on the nature of the substrate. *Biotechnol. Bioeng. 86*, 503−511.
(17) Teugjas, H., and Väljamäe, P. (2013) Product inhibition of cellulases studied with C-14-labeled cellulose substrates. *Biotechnol. Biofuels 6*, No. 10.1186/1754-6834-6-104.
(18) Bansal, P., Hall, M., Realff, M. J., Lee, J. H., and Bommarius, A. S. (2009) Modeling cellulase kinetics on lignocellulosic substrates. *Biotechnol. Adv. 27*, 833−848.
(19) Igarashi, K., Koivula, A., Wada, M., Kimura, S., Penttila, M., and Samejima, M. (2009) High Speed Atomic Force Microscopy Visualizes Processive Movement of Trichoderma reesei Cellobiohydrolase I on Crystalline Cellulose. *J. Biol. Chem. 284*, 36186−36190.
(20) Igarashi, K., Uchihashi, T., Koivula, A., Wada, M., Kimura, S., Okamoto, T., Penttila, M., Ando, T., and Samejima, M. (2011) Traffic Jams Reduce Hydrolytic Efficiency of Cellulase on Cellulose Surface. *Science 333*, 1279−1282.
(21) Kurasin, M., and Väljamäe, P. (2011) Processivity of Cellobiohydrolases Is Limited by the Substrate. *J. Biol. Chem. 286*, 169−177.
(22) Jalak, J., Kurasin, M., Teugjas, H., and Väljamäe, P. (2012) Endo-exo Synergism in Cellulose Hydrolysis Revisited. *J. Biol. Chem. 287*, 28802−28815.
(23) Kipper, K., Väljamäe, P., and Johansson, G. (2005) Processive action of cellobiohydrolase Cel7A from Trichoderma reesei is revealed as 'burst' kinetics on fluorescent polymeric model substrates. *Biochem. J. 385*, 527−535.
(24) von Ossowski, I., Ståhlberg, J., Koivula, A., Piens, K., Becker, D., Boer, H., Harle, R., Harris, M., Divne, C., Mahdi, S., Zhao, Y. X., Driguez, H., Claeyssens, M., Sinnott, M. L., and Teeri, T. T. (2003) Engineering the exo-loop of Trichoderma reesei cellobiohydrolase, Ce17A. A comparison with Phanerochaete chrysosporium Cel7D. *J. Mol. Biol. 333*, 817−829.
(25) Fox, J. M., Levine, S. E., Clark, D. S., and Blanch, H. W. (2012) Initial- and Processive-Cut Products Reveal Cellobiohydrolase Rate Limitations and the Role of Companion Enzymes. *Biochemistry 51*, 442−452.
(26) Maurer, S. A., Bedbrook, C. N., and Radke, C. J. (2012) Cellulase Adsorption and Reactivity on a Cellulose Surface from Flow Ellipsometry. *Ind. Eng. Chem. Res. 51*, 11389−11400.
(27) Wilson, D. B. (2009) Cellulases and biofuels. *Curr. Opin. Biotechnol. 20*, 295−299.
(28) Shang, B. Z., Chang, R., and Chu, J. (2013) Systems-level modeling with molecular resolution elucidates the rate-limiting mechanisms of cellulose decomposition by cellobiohydrolases. *J. Biol. Chem.*, No. 10.1074/jbc.M1113.497412.
(29) Jalak, J., and Väljamäe, P. (2010) Mechanism of Initial Rapid Rate Retardation in Cellobiohydrolase Catalyzed Cellulose Hydrolysis. *Biotechnol. Bioeng. 106*, 871−883.
(30) Gao, D., Chundawata, S. P. S., Sethic, A., Balana, V., Gnanakaranc, S., and Dale, B. E. (2013) Increased enzyme binding to substrate is not necessary for more efficient cellulose hydrolysis. *Proc. Natl. Acad. Sci. U. S. A. 110*, 10922−10927.
(31) Beckham, G. T., Matthews, J. F., Peters, B., Bomble, Y. J., Himmel, M. E., and Crowley, M. F. (2011) Molecular-Level Origins of Biomass Recalcitrance: Decrystallization Free Energies for Four Common Cellulose Polymorphs. *J. Phys. Chem. B 115*, 4118−4127.
(32) Himmel, M. E., Ding, S. Y., Johnson, D. K., Adney, W. S., Nimlos, M. R., Brady, J. W., and Foust, T. D. (2007) Biomass recalcitrance: Engineering plants and enzymes for biofuels production. *Science 315*, 804−807.
(33) Chundawat, S. P. S., Beckham, G. T., Himmel, M. E., and Dale, B. E. (2011) Deconstruction of Lignocellulosic Biomass to Fuels and Chemicals in *Annual Review of Chemical and Biomolecular Engineering*, Vol 2 (Prausnitz, J. M., Ed.); Annual Reviews: Palo Alto, CA, pp 121-145.
(34) Kostylev, M., Moran-Mirabal, J. M., Walker, L. P., and Wilson, D. B. (2012) Determination of the molecular states of the processive endocellulase Thermobifida fusca Cel9A during crystalline cellulose depolymerization. *Biotechnol. Bioeng. 109*, 295−299.
(35) Bansal, P., Vowell, B. J., Hall, M., Realff, M. J., Lee, J. H., and Bommarius, A. S. (2012) Elucidation of cellulose accessibility, hydrolysability and reactivity as the major limitations in the enzymatic hydrolysis of cellulose. *Bioresour. Technol. 107*, 243−250.
(36) Arantes, V., and Saddler, J. N. (2010) Access to cellulose limits the efficiency of enzymatic hydrolysis: the role of amorphogenesis. *Biotechnol. Biofuels 3*, 11.
(37) Hall, M., Bansal, P., Lee, J. H., Realff, M. J., and Bommarius, A. S. (2011) Biological pretreatment of cellulose: Enhancing enzymatic hydrolysis rate using cellulose-binding domains from cellulases. *Bioresour. Technol. 102*, 2910−2915.
(38) Guo, J., and Catchmark, J. M. (2013) Binding Specificity and Thermodynamics of Cellulose-Binding Modules from Trichoderma reesei Cel7A and Cel6A. *Biomacromolecules 14*, 1268−1277.
(39) Tomme, P., Vantilbeurgh, H., Pettersson, G., Vandamme, J., Vandekerckhove, J., Knowles, J., Teeri, T., and Claeyssens, M. (1988) Studies of the cellulolytic system of trichoderma-reesei QM-9414 - Analysis of domian function in2 cellobiohydrolases by limitied proteolysis. *Eur. J. Biochem. 170*, 575−581.
(40) Lucius, A. L., Maluf, N. K., Fischer, C. J., and Lohman, T. M. (2003) General methods for analysis of sequential "n-step" kinetic mechanisms: Application to single turnover kinetics of helicase-catalyzed DNA unwinding. *Biophys. J. 85*, 2224−2239.
(41) Jung, J., Sethi, A., Gaiotto, T., Jeoh, T., Gnanakaran, S., and Goodwin, P. M. (2013) Binding and movement of individual Cel7A cellobiohydrolases on crystalline cellulose surfaces revealed by single-molecule fluorescence imaging. *J. Biol. Chem.*, No. 10.1074/jbc.M113.455758.
(42) Väljamäe, P., Kipper, K., Pettersson, G., and Johansson, G. (2003) Synergistic cellulose hydrolysis can be described in terms of fractal-like kinetics. *Biotechnol. Bioeng. 84*, 254−257.
(43) Xu, F., and Ding, H. S. (2007) A new kinetic model for heterogeneous (or spatially confined) enzymatic catalysis: Contributions from the fractal and jamming (overcrowding) effects. *Appl. Catal., A 317*, 70−81.
(44) Kostylev, M., and Wilson, D. B. (2013) Two-Parameter Kinetic Model Based on a Time-Dependent Activity Coefficient Accurately Describes Enzymatic Cellulose Digestion. *Biochemistry 52*, 5656−5664.
(45) Azizian, S. (2004) Kinetic models of sorption: a theoretical analysis. *J. Colloid Interface Sci. 276*, 47−52.
(46) Fall, A. B., Lindstrom, S. B., Sundman, O., Odberg, L., and Wagberg, L. (2011) Colloidal Stability of Aqueous Nanofibrillated Cellulose Dispersions. *Langmuir 27*, 11332−11338.
(47) Wang, W., Kang, L., Wei, H., Arora, R., and Lee, Y. Y. (2011) Study on the Decreased Sugar Yield in Enzymatic Hydrolysis of

Cellulosic Substrate at High Solid Loading. *Appl. Biochem. Biotechnol. 164*, 1139−1149.
(48) Beldman, G., Voragen, A. G. J., Rombouts, F. M., Searlevanleeuwen, M. F., and Pilnik, W. (1987) Adsorption and Kinetic-Behavior of Purified Endoglucanases and Exoglucanases from Trichoderma-Viride. *Biotechnol. Bioeng. 30*, 251−257.